

PHOTOCATALYTIC PERFORMANCE OF A SLURRY AND
IMMOBILIZED TiO₂ DEGUSSA P-25 FOR THE DEGRADATION OF
AQUEOUS ORGANIC POLLUTANTS UNDER 45W COMPACT
FLUORESCENT LAMP

by

SALMIAH MD ZAIN

Thesis submitted in fulfilment of the requirements
for the degree of
Master of Science

February 2012

ACKNOWLEDGEMENTS

In the name of God, the most compassionate, the most merciful. Hereby, I would like to convey my utmost appreciation to individuals that assisted and supported me directly or indirectly in completing this thesis. First and foremost, I would like to thank my supervisor Professor Dr. Hj. Mohd Asri Mohd Nawi for his outstanding guidance, invaluable advice and encouragement throughout my candidature.

I would also like to extend my special thanks to Ministry of Higher Education for the scholarship given under Biasiswa Bajet Mini and to Universiti Sains Malaysia for the Graduate Assistant scheme and Research University-Postgraduate Research Grant Scheme (RU-PRGS: 1001/PKIMIA/832058).

My gratitude also goes to all the administrative and technical staff of School of Chemical Sciences, School of Biological Sciences and Institute of Postgraduate Studies USM for their contributions and assistance throughout my research especially for the handling of various types of analytical equipments.

Lastly, my sincere appreciation goes to all members of Photocatalysis Laboratory, lecturers and friends for their encouragement and supports. Lastly, I would like to pass along my very special thanks to my parents and family for their patience, continuous blessings and support during the challenging times. Thank You.

TABLE OF CONTENTS

	Page
Acknowledgements	ii
Table of Contents	iii
List of Figures	x
List of Tables	xvi
List of Plates	xvii
List of Abbreviations	xviii
Abstrak	xix
Abstract	xxi

CHAPTER 1 – INTRODUCTION

1.1	An Overview	1
1.2	Organic Pollutants in Wastewater	3
1.2.1	Coloured wastewater	3
1.2.1.1	Reactive Red 4, RR4	5
1.2.1.2	Methylene Blue, MB	6
1.2.2	Phenol compounds	7
1.3	Decomposition of Organic Pollutants in Wastewater	9
1.3.1	Wastewater treatment methods	9
1.3.2	AOP methods	12
1.3.2.1	Non-photochemical processes	13
1.3.2.2	Photochemical processes	14
1.4	Fundamentals of Heterogeneous Photocatalysis	16

1.4.1	Photocatalysts	18
1.4.2	Titanium dioxide (TiO ₂) as a semiconductor	21
1.4.2.1	Historical background	21
1.4.2.2	Structural and photocatalytic properties of TiO ₂	22
1.4.2.3	Titanium Dioxide Degussa P-25	24
1.5	Mechanism of Photocatalytic Oxidation Process	25
1.6	Langmuir-Hinshelwood Isotherm	28
1.7	Immobilization of P-25 Powder	30
1.8	Improving Efficiency of Photocatalyst	41
1.9	Polymer Blend	43
1.9.1	Epoxidized natural rubber, ENR	45
1.9.2	Poly (vinyl chloride), PVC	46
1.9.3	ENR/PVC blends	48
1.10	Problem Statement and Research Objectives	48

CHAPTER 2 – EXPERIMENTAL

2.1	Chemicals and Reagents	51
2.2	Instruments and Equipments	52
2.3	Preparation of Samples Solutions	53
2.3.1	RR4	53
2.3.2	MB	53
2.3.3	Phenol	54
2.4	Fabrications of Immobilized P-25/ENR/PVC Catalyst onto Glass Plates	54
2.4.1	Preparation of ENR solution	54
2.4.2	Determination of the amount of ENR in toluene	54

2.4.3	Optimization of ENR to PVC ratio in P-25/ENR/PVC formulation	55
2.4.3.1	Optimization of PVC in P-25/ENR/PVC formulation	55
2.4.3.2	Optimization of ENR in P-25/ENR/PVC formulation	56
2.4.4	Fabrication of immobilized P-25/ENR/PVC plates	57
2.5	Characterization of P-25/ENR/PVC Catalyst	59
2.6	Reactor Setup for Photocatalytic Process	59
2.7	Decomposition of RR4, MB and Phenol	60
2.7.1	Photolysis	61
2.7.2	Photocatalytic and adsorption study using immobilized catalyst	61
2.7.3	Photocatalytic and adsorption study using slurry or suspended catalyst	62
2.8	Analytical Procedures	63
2.9	Adhesion of Immobilized P-25/ENR/PVC Layer on Glass Plate	63
2.10	Degradation of Polymer Blend within Immobilized P-25/ENR/PVC Layer	64
2.10.1	COD test	64
2.10.1.1	Preparation of COD reagent	64
2.10.1.2	Standardization of prepared COD reagent	65
2.10.1.3	Preparation of COD sample	66
2.10.1.4	Reflux process and the measurement of COD concentration	67
2.10.2	Ion Chromatography (IC) Analysis	67
2.10.2.1	Measurement of Cl ⁻ ion concentration	67
2.10.3	SEM analysis	68
2.10.4	TGA analysis	69

2.10.5	FTIR analysis	69
2.10.6	BET analysis	69
2.10.7	CHN analysis	70
2.11	Enhancement of Surface Area of the Immobilized P-25/ENR/PVC/5h System and the Optimization of Operational Parameters for the Degradation of RR4	70
2.11.1	Effect of photocatalyst loading	71
2.11.2	Effect of pH	71
2.11.2.1	Determination of point of zero charge (pH_{pzc}) for P-25/ENR/PVC photocatalyst	71
2.11.2.2	Effect of initial pH of RR4 dye solution	72
2.11.3	Effect of aeration rates	72
2.11.4	Effect of initial concentration of RR4	72
2.11.5	Reusability and stability of the immobilized catalyst	73
2.12	Mineralization Study	73
2.12.1	COD removal of RR4, MB and Phenol	74
2.12.2	Monitoring of pH changes of the treated RR4, MB and Phenol solutions	74
2.12.3	Detection of inorganic ions (Cl^- , SO_4^{2-} and NO_3^-) from the mineralization of RR4 and MB solutions using IC	74

CHAPTER 3 – RESULT AND DISCUSSION

3.1	Preparation of the P-25/ENR/PVC Dip-coating Formulation	75
3.1.1	Optimizing the amount of ENR in P-25/ENR/PVC dip-coating formulation	75

3.1.2	Optimization of the PVC content in P-25/ENR/PVC dip-coating formulation	78
3.1.3	Characterization of P-25/ENR/PVC formulation	83
3.1.3.1	SEM analysis	83
3.1.3.2	BET analysis	86
3.1.3.3	FTIR analysis	87
3.1.4	Organic matter leaching test of the ENR/PVC blend	90
3.1.5	Surface morphology of the catalyst after degradation of polymer blend	94
3.1.6	Thermogravimetric analysis of catalyst	97
3.1.7	FTIR analysis of the irradiated immobilized P-25/ENR/PVC photocatalyst	103
3.1.8	BET analysis of the irradiated immobilized P-25/ENR/PVC photocatalyst	105
3.1.9	The weight loss of immobilized P-25/ENR/PVC catalyst due to prolong irradiation.	106
3.1.10	CHN analysis of the irradiated immobilized P-25/ENR/PVC/5h photocatalyst	108
3.2	Photocatalytic Degradation of RR4 Dyes by Immobilized P-25/ENR/PVC Photocatalyst	110
3.2.1	Comparison of photocatalytic performances between slurry and immobilized mode of applications of the photocatalysts.	110
3.2.2	Influence of operational parameters on the photocatalytic degradation of RR4 dyes	116
3.2.2.1	Effect of aeration rate	117

3.2.2.2	Catalyst loading	120
3.2.2.3	Initial pH solution	124
3.2.2.4	The effect of initial concentrations of RR4 dye solutions	127
3.2.3	Reusability and sustainability of the P-25/ENR/PVC/5h photocatalyst during the photocatalytic degradation of RR4 dyes	130
3.2.4	Mineralization of RR4 dye	134
3.2.4.1	Temporal change and the COD evaluation of the photocatalytic degradation of RR4 dye solution	135
3.2.4.2	pH evolution during RR4 mineralization process	138
3.2.4.3	Detection of anions compounds (Cl^- , SO_4^{2-} , and NO_3^-)	140
3.3	MB as the Cationic Model Pollutant	148
3.3.1	Photocatalytic degradation of MB	148
3.3.2	Reusability and sustainability of immobilized P-25/ENR/PVC/5h in the photocatalytic degradation of MB dyes	153
3.3.3	Mineralization of MB dye	157
3.3.3.1	Temporal change of MB upon photodegradation and its COD evaluation	157
3.3.3.2	Detection of ions (SO_4^{2-} , NO_3^- , and H^+)	158
3.4	Comparison of the Photocatalytic Degradation of an Anionic and a Cationic Dye	164
3.5	Phenol as the Neutral Model Pollutant	167
3.5.1	Photocatalytic degradation of phenol	167
3.5.2	Reusability and sustainability of phenol	172
3.5.3	Mineralization of Phenol	174
3.5.3.1	Temporal change of phenol upon photocatalytic	

degradation and its COD and pH evaluation	175
---	-----

CHAPTER 4 – CONCLUSION AND RECOMMENDATIONS

4.1 Conclusion	178
4.2 Recommendations	183

REFERENCES	185
-------------------	-----

APPENDICES

Appendix A	Linearity of $\ln C_0/C$ versus irradiation time for photocatalytic degradation of RR4 at different amount of ENR added	202
Appendix B	Experimental data for determination of the ratio of ENR to solvent	203
Appendix C	The nitrogen adsorption-desorption isotherm	204
Appendix D	Theoretical concentration of inorganic ions in degradation of RR4 and MB dyes	206
Appendix E	List of publication, seminars/conferences	208

LIST OF FIGURES

		Page
Figure 1.1	Molecular structure of RR4 dye	5
Figure 1.2	Molecular structure of MB	7
Figure 1.3	The conduction and valence band positions of the selected semiconductors at pH 0. [Picture adapted from 47, 48]	19
Figure 1.4	The simplified mechanism for the photoactivation of photocatalysts [52]	28
Figure 1.5	Epoxidation of natural rubber [108]	45
Figure 2.1	Steps of a dip coating process	58
Figure 2.2	Scheme of experimental setup	60
Figure 3.1	The percentage of immobilized P-25/ENR/PVC catalyst remaining on the glass plates after 30 s of sonication with 40 kHz ultra sonic cleaner. Immobilized P-25/ENR/PVC catalyst plates were fabricated using different amount of ENR and fixed amount of PVC inside P-25/ENR/PVC formulation.	79
Figure 3.2	Pseudo-first order rate constants for different amount of PVC in P-25/ENR/PVC formulations from the photocatalytic degradation and adsorption processes of 15 mg L ⁻¹ of RR4 dye.	81
Figure 3.3	The percentage of immobilized P-25/ENR/PVC that remained on the glass plates during 30 s of sonication using 40 kHz ultra sonic cleaner. Immobilized P-25/ENR/PVC plates were fabricated with different amount of PVC and fixed amount of ENR added into the P-25/ENR/PVC formulation.	83
Figure 3.4	Scanning electron micrograph of the surface of unmodified P-25 powder (30K magnification)	84
Figure 3.5	Scanning electron micrograph of the surface of immobilized P-25/ENR/PVC at high magnification (30K magnification)	85

Figure 3.6	Scanning electron micrograph of the surface of P-25/ENR/PVC at low magnification (5K magnification)	85
Figure 3.7	The FTIR spectra for the catalyst (a) P-25 powder, and immobilized systems of (b) P-25/PVC, (c) P-25/ENR and (d) P-25/ENR/PVC	89
Figure 3.8	COD concentration of treated water samples irradiated under fluorescent lamp in the presence of immobilized P-25/PVC, P-25/ENR, and P-25/ENR/PVC over the span of 10 h	92
Figure 3.9	Concentration of chloride ions in treated water sample irradiated under fluorescent lamp in the presence of immobilized P-25/ENR/PVC plate over the span of 10 h.	93
Figure 3.10	SEM micrographs of optimized formulation (a) P-25/ENR/PVC before irradiation (5K magnification) and P-25/ENR/PVC after (b) 3 (5K magnification), (c) 5 (10K magnification), and (d) 10 h (10K magnification) of irradiation under fluorescent light.	95
Figure 3.11	TG and DTG profile of ENR	99
Figure 3.12	TG and DTG profile of PVC	99
Figure 3.13	TG and DTG profiles of the immobilized P-25/ENR/PVC before irradiation and P-25/ENR/PVC after 3, 5, 8, and 10 h of irradiation plate under fluorescent lamp.	100
Figure 3.14	The comparison of FTIR spectrum for the immobilized (a) P-25/ENR/PVC before irradiation and P-25/ENR/PVC after (b) 1, (c) 3, and (d) 10 h of irradiation under fluorescent lamp.	104
Figure 3.15	The percentage of P-25/ENR/PVC remains under illumination of light in ultra pure water	108
Figure 3.16	Percentage colour remaining of RR4 dye by using photolysis, P-25 slurry system, and immobilized P-25/ENR/PVC and P-25/ENR/PVC/5h catalyst plate (Experimental condition: P-25 powder & P-25/ENR/PVC coating : $1.500 \pm 0.005 \text{ mg cm}^{-2}$, $[\text{RR4}]_0$: 15 mg L^{-1} , aeration rate: 40 mL min^{-1} , initial pH_{RR4} : 6.2)	112

Figure 3.17	Pseudo-first order rate constants for the degradation of RR4 dye via photocatalysis and adsorption processes using P-25 slurry system, and immobilized P-25/ENR/PVC and P-25/ENR/PVC/5h catalyst plate. (Experimental condition: P-25 powder & P-25/ENR/PVC: $1.500 \pm 0.005 \text{ mg cm}^{-2}$, $[\text{RR4}]_0$: 15 mg L^{-1} , aeration rate: 40 mL min^{-1} , initial pH_{RR4} : 6.2)	115
Figure 3.18	Pseudo-first order rate constants at different aeration flow rate used during the photocatalytic degradation and adsorption of RR4 by the optimized P-25/ENR/PVC/5h catalyst plate. (Experimental condition: P-25/ENR/PVC/5h: $1.1 \pm 0.005 \text{ mg cm}^{-2}$, $[\text{RR4}]_0$: 15 mg L^{-1} , initial pH_{RR4} : 6.2)	119
Figure 3.19	Pseudo-first order rate constants for different amount of catalyst loading of the optimized P-25/ENR/PVC/5h catalyst plate via photocatalysis and adsorption of RR4. (Experimental condition: $[\text{RR4}]_0$: 15 mg L^{-1} , aeration rate: 40 mL min^{-1} , initial pH_{RR4} : 6.2)	123
Figure 3.20	Pseudo-first order rate constants for decolourization of RR4 dye at different initial pH values by optimized P-25/ENR/PVC/5h catalyst plate via photocatalysis and adsorption process. (Experimental condition: P-25/ENR/PVC/5h: $1.500 \pm 0.005 \text{ mg cm}^{-2}$, $[\text{RR4}]_0$: 15 mg L^{-1} , aeration rate: 40 mL min^{-1})	126
Figure 3.21	Pseudo-first order rate constants for decolourization of RR4 dye at different initial concentration by the optimized P-25/ENR/PVC/5h catalyst plate via photocatalysis and adsorption processes. (Experimental condition: P-25/ENR/PVC/5h: $1.500 \pm 0.005 \text{ mg cm}^{-2}$, initial pH_{RR4} : 6.2, aeration rate: 40 mL min^{-1})	129
Figure 3.22	Pseudo-first order rate constant for photocatalytic degradation of RR4 dye up to 3 cycles of repeated applications with different washing time process. (Experimental condition: m (P-25/ENR/PVC/5h): $1.500 \pm 0.005 \text{ mg cm}^{-2}$, $[\text{RR4}]_0$: 15 mg L^{-1} , pH_{RR4} : 6.2, aeration rate: 40 mL min^{-1})	132
Figure 3.23	The comparison of pseudo-first order rate constants and percentage removal of RR4 by photocatalytic degradation up to 10 cycles of repeated applications of P-25/ENR/PVC/5h when 15 and 30 min washing time were applied in between the cycle. (Experimental condition: m (P-25/ENR/PVC/5h): $1.500 \pm 0.005 \text{ mg cm}^{-2}$, $[\text{RR4}]_0$: 15	133

mg L⁻¹, pH_{RR4}: 6.2, aeration rate: 40 mL min⁻¹)

- Figure 3.24 Percentage of decolorization and COD removal of the RR4 solution by using P-25 powder and immobilized P-25/ENR/PVC/5h catalyst plate. (Experimental condition: P-25 powder and P-25/ENR/PVC/5h: 1.500 ± 0.005 mg cm⁻², [RR4]_o: 30 mg L⁻¹, initial pH_{RR4}: 7.07, aeration rate: 40 mL min⁻¹) 137
- Figure 3.25 pH evolution during the photocatalytic degradation of RR4 dye by suspended P-25 powder and immobilized P-25/ENR/PVC/5h catalyst (Experimental condition: P-25 powder and P-25/ENR/PVC/5h: 1.500 ± 0.005 mg cm⁻², [RR4]_o: 30 mg L⁻¹, initial pH_{RR4}: 7.07, aeration rate: 40 mL min⁻¹) 139
- Figure 3.26 Evolution of chloride ions in RR4 solution treated by suspended P-25 powder and immobilized P-25/ENR/PVC/5h catalyst under irradiation by 45 W fluorescent lamp (Experimental condition: m (P-25 powder and P-25/ENR/PVC/5h): 1.500 ± 0.005 mg cm⁻², [RR4]_o: 30 mg L⁻¹, pH_{RR4}: 7.07, aeration rate: 40 mL min⁻¹) 142
- Figure 3.27 Evolution of sulphate ions in RR4 solution treated by suspended P-25 powder and immobilized P-25/ENR/PVC/5h catalyst under irradiation of 45 watt fluorescent lamp (Experimental condition: P-25 powder and P-25/ENR/PVC/5h: 1.500 ± 0.005 mg cm⁻², [RR4]_o: 30 mg L⁻¹, initial pH_{RR4}: 7.07, aeration rate: 40 mL min⁻¹) 143
- Figure 3.28 Evolution of nitrate ions in RR4 solution treated by suspended P-25 powder and immobilized P-25/ENR/PVC/5h catalyst under irradiation of 45 watt fluorescent lamp (Experimental condition: P-25 powder and P-25/ENR/PVC/5h: 1.500 ± 0.005 mg cm⁻², [RR4]_o: 30 mg L⁻¹, initial pH_{RR4}: 7.07, aeration rate: 40 mL min⁻¹) 147
- Figure 3.29 Percentage colour removal of MB by photolysis, P-25 slurry system, and immobilized P-25/ENR/PVC and P-25/ENR/PVC/5h catalyst plate (Experimental condition: P-25 powder & P-25/ENR/PVC: 1.500 ± 0.005 mg cm⁻², [MB]_o: 12 mg L⁻¹, aeration rate: 40 mL min⁻¹, initial pH_{MB}: 7.6) 149
- Figure 3.30 Pseudo-first order rate constants for the removal of MB dye via photocatalysis and adsorption processes using P-25 slurry system, and immobilized P-25/ENR/PVC and P- 151

25/ENR/PVC/5h catalyst plate. (Experimental condition: P-25 powder & P-25/ENR/PVC: $1.500 \pm 0.005 \text{ mg cm}^{-2}$, $[\text{MB}]_0$: 12 mg L^{-1} , aeration rate: 40 mL min^{-1} , initial pH_{MB} : 7.6)

- Figure 3.31 Pseudo-first order rate constants for the photocatalytic degradation of MB up to 10 cycles of repeated applications. (Experimental condition: P-25/ENR/PVC/5h: $1.500 \pm 0.005 \text{ mg cm}^{-2}$, $[\text{MB}]_0$: 12 mg L^{-1} , pH_{MB} : 7.6, aeration rate: 40 mL min^{-1}) 154
- Figure 3.32 Percentage of MB remains after each cycle of photocatalytic degradation of the dye up to 10 cycles of repeated applications. (Experimental condition: P-25/ENR/PVC/5h: $1.500 \pm 0.005 \text{ mg cm}^{-2}$, $[\text{MB}]_0$: 12 mg L^{-1} , initial pH_{MB} : 7.6, aeration rate: 40 mL min^{-1}) 156
- Figure 3.33 Percentage decolorization and COD removal of the MB solution by the photocatalytic degradation using P-25 powder and immobilized P-25/ENR/PVC/5h catalyst plate. (Experimental condition: P-25 powder and P-25/ENR/PVC/5h: $1.500 \pm 0.005 \text{ mg cm}^{-2}$, $[\text{MB}]_0$: 20 mg L^{-1} , initial pH_{MB} : 7.93, aeration rate: 40 mL min^{-1}) 159
- Figure 3.34 Evolution of sulphate and nitrate ions in the treated MB solution by suspended P-25 powder and immobilized P-25/ENR/PVC/5h catalyst under irradiation by 45 watt fluorescent lamp (Experimental condition: P-25 powder and P-25/ENR/PVC/5h: $1.500 \pm 0.005 \text{ mg cm}^{-2}$, $[\text{MB}]_0$: 20 mg L^{-1} , initial pH_{MB} : 7.93, aeration rate: 40 mL min^{-1}) 162
- Figure 3.35 pH evolution during the photocatalytic degradation of MB dye by suspended P-25 powder and immobilized P-25/ENR/PVC/5h catalyst (Experimental condition: P-25 powder and P-25/ENR/PVC/5h: $1.500 \pm 0.005 \text{ mg cm}^{-2}$, $[\text{MB}]_0$: 20 mg L^{-1} , initial pH_{MB} : 7.93, aeration rate: 40 mL min^{-1}) 163
- Figure 3.36 Percentage of phenol remaining after treatments using photolysis, P-25 slurry system, and immobilized P-25/ENR/PVC and P-25/ENR/PVC/5h catalyst plate (Experimental condition: P-25 powder & P-25/ENR/PVC: $1.500 \pm 0.005 \text{ mg cm}^{-2}$, $[\text{Phenol}]_0$: 10 mg L^{-1} , aeration rate: 40 mL min^{-1} , initial $\text{pH}_{\text{phenol}}$: 6.5) 169

Figure 3.37	Comparison of pseudo-first order rate constants and percentage decomposition of phenol via photocatalysis and adsorption process using P-25 slurry system, and immobilized P-25/ENR/PVC and P-25/ENR/PVC/5h catalyst plate. (Experimental condition: P-25 powder, P-25/ENR/PVC & P-25/ENR/PVC/5h: $1.500 \pm 0.005 \text{ mg cm}^{-2}$, $[\text{Phenol}]_0$: 10 mg L^{-1} , aeration rate: 40 mL min^{-1} , initial $\text{pH}_{\text{phenol}}$: 6.5)	170
Figure 3.38	Percentage decomposition for photocatalytic degradation of phenol up to three cycles of repeated applications. (Experimental condition: P-25/ENR/PVC/5h: $1.500 \pm 0.005 \text{ mg cm}^{-2}$, $[\text{Phenol}]_0$: 10 mg L^{-1} , initial $\text{pH}_{\text{phenol}}$: 6.5, aeration rate: 40 mL min^{-1})	173
Figure 3.39	Pseudo-first order rate constants for the photocatalytic degradation of phenol for three cycles of repeated applications. (Experimental condition: P-25/ENR/PVC/5h: $1.500 \pm 0.005 \text{ mg cm}^{-2}$, $[\text{Phenol}]_0$: 10 mg L^{-1} , initial $\text{pH}_{\text{phenol}}$: 6.5, aeration rate: 40 mL min^{-1})	173
Figure 3.40	Percentage decomposition and COD removal of the phenol solution during its photodegradation by using P-25 powder and immobilized P-25/ENR/PVC/5h catalyst plate. (Experimental condition: P-25 powder & P-25/ENR/PVC/5h: $1.500 \pm 0.005 \text{ mg cm}^{-2}$, $[\text{Phenol}]_0$: 20 mg L^{-1} , initial $\text{pH}_{\text{phenol}}$: 7.70, aeration rate: 40 mL min^{-1})	176
Figure 3.41	pH evolution during the photocatalytic degradation of phenol by suspended P-25 powder and immobilized P-25/ENR/PVC/5h catalyst (Experimental condition: P-25 powder & P-25/ENR/PVC/5h: $1.500 \pm 0.005 \text{ mg cm}^{-2}$, $[\text{Phenol}]_0$: 20 mg L^{-1} , initial $\text{pH}_{\text{phenol}}$: 7.72, aeration rate: 40 mL min^{-1})	177

LIST OF TABLES

		Page
Table 1.1	An established and emerging AOP methods [36]	13
Table 1.2	Summary of the application of immobilized photocatalyst in heterogeneous photocatalysis	35
Table 3.1	The average pseudo-first order rate constant for the degradation of RR4 dye and the COD concentration of the P-25/ENR/PVC catalyst plate with different amount of ENR and fixed amount of PVC	76
Table 3.2	BET result for P-25 powder and immobilized P-25/ENR/PVC plate	87
Table 3.3	Thermogravimetric data of ENR, PVC, before, and after irradiation of immobilized P-25/ENR/PVC catalyst	101
Table 3.4	BET result for immobilized P-25/ENR/PVC and P-25/ENR/PVC/5h	105
Table 3.5	CHN result for immobilized P-25/ENR/PVC and P-25/ENR/PVC/5h	109
Table 3.6	Point of zero charge (pHpzc) for P-25 powder and the immobilized P-25/ENR/PVC/5h catalyst plate	124
Table 3.7	Photodegradation ratio and pseudo-first order rate constant (photocatalysis) of RR4 and MB dye within 1 h or irradiation using immobilized P-25/ENR/PVC/5h catalyst plate (Experimental condition: P-25/ENR/PVC: $1.500 \pm 0.005 \text{ mg cm}^{-2}$)	165

LIST OF PLATES

		Page
Plate 3.1	Glass plate freshly coated with P-25/ENR/PVC formulation	107
Plate 3.2	Glass plate coated with P-25/ENR/PVC formulation after 5 h of irradiation	107

LIST OF ABBREVIATIONS

AOPs	Advanced Oxidation Processes
BET	Brunner-Emmet Teller
CHN	Carbon, Hydrogen, Nitrogen
COD	Chemical Oxygen Demand
e^-	Negatively charged electron
ENR	Epoxidized Natural Rubber
FTIR	Fourier Transform Infra Red
h	Hour
h^+	Positively charged hole
L-H	Langmuir-Hinshelwood
MB	Methylene Blue
min	Minute
pH_{pzc}	pH at point of zero charge
PVC	Poly (vinyl) chloride
RR4	Reactive Red 4
SEM	Scanning Electron Microscopy
TGA	Thermogravimetric Analysis
UV	Ultra Violet
W	Watt

**PRESTASI PEMFOTOMANGKIN TiO₂ DEGUSSA P-25 TERAMPAI DAN
TERIMMOBILISASI UNTUK PENGURAIAN BAHAN PENCEMAR
ORGANIK AKUEUS DI BAWAH SINARAN LAMPU PADAT
BERPENDARFLOUR 45 W**

ABSTRAK

Kaedah penyaduran celup yang ringkas dan berkesan telah digunakan untuk mengimmobilisasikan serbuk P-25 pada permukaan plat kaca dengan menggunakan adunan polimer getah asli terepoksi (ENR)/ poli vinil klorida (PVC) sebagai pelekat. Kebolegunaan semula plat P-25/ENR/PVC dapat mengelakkan daripada langkah penapisan yang merumitkan didalam sistem larutan akueus terampai. Berdasarkan pada kadar penyingkiran warna RR4 dan kadar kemelekatan formulasi P-25, nisbah optimum ENR kepada PVC adalah 1:2. Plat terimmobilisasi P-25/ENR/PVC telah dicirikan menggunakan SEM, TGA, dan BET. Disebabkan oleh daya tahan yang rendah, organik polimer ENR dan PVC yang digunakan dalam sistem ini mudah mengurai dan mengakibatkan penghasilan keperluan oksigen kimia (COD) dalam air ultra tulen terawat. Prosedur mencuci melalui proses penyinaran dapat menstabilkan penguraian polimer dan meningkatkan luas permukaan mangkin terimmobilisasi. pH awal larutan RR4, kuantiti pemangkin, aliran udara, dan kepekatan awal larutan RR4 didapati mempengaruhi pemalar kadar tertib pseudo-pertama aktiviti pemfotomangkin RR4. Kehadiran aliran udara sebagai sumber oksigen meningkatkan kadar penguraian pemfotomangkin. Muatan optimum mangkin adalah sebanyak $1.500 \pm 0.005 \text{ mg cm}^{-2}$ dan kadar penguraian pemfotomangkin RR4 adalah paling tinggi dalam keadaan asid. Peningkatan kepekatan awal larutan pewarna RR4 menyebabkan berlaku penurunan kadar penguraian. Peranan penjerapan dan struktur

kimia bahan pencemar organik juga mempengaruhi kadar aktiviti penguraian. Kadar penguraian RR4 dan fenol adalah lebih perlahan dengan menggunakan sistem terimmobilisasi. Walau bagaimanapun, kadar penguraian MB menggunakan plat terimmobilisasi P-25/ENR/PVC/5h adalah lebih baik berbanding dengan pemfotomangkin dalam mod ampaian. Plat terimmobilisasi P-25 boleh diulang guna semula untuk banyak kitaran aplikasi. Tahap mineralisasi bahan pencemar organik juga dinilai dengan mengukur COD, kadar perubahan pH, dan evolusi ion nitrat, sulfat dan klorida terhadap bahan pencemar. Penguraian warna RR4 dan MB didapati lebih cepat berbanding proses mineralisasi, tetapi kadar penguraian fenol pula didapati hampir sama dengan kadar mineralisasinya.

PHOTOCATALYTIC PERFORMANCE OF A SLURRY AND IMMOBILIZED TiO₂ DEGUSSA P-25 FOR THE DEGRADATION OF AQUEOUS ORGANIC POLLUTANTS UNDER 45W COMPACT FLUORESCENT LAMP

ABSTRACT

A simple and effective dip coating method was used for immobilizing P-25 powder onto glass plates using epoxidized natural rubber (ENR)/ poly (vinyl) chloride (PVC) blend as adhesives. The reusable P-25/ENR/PVC catalyst plate could avoid tedious filtration step in aqueous slurry system. Based on the photocatalytic removal rate of RR4 and the adhesion of the P-25 formulation, the optimum ratio of ENR to PVC for the immobilization was determined as 1:2. The immobilized P-25/ENR/PVC catalyst plate was characterized using SEM, TGA and BET analyses. Due to the low durability of the organic polymer, ENR and PVC applied in this system were prone to be degraded and resulted in the detection of chemical oxygen demand (COD) values in the treated ultrapure water. By washing procedure through irradiation process could stabilize the polymer blend and increase the BET surface area of the immobilized catalyst. The initial pH of RR4 solution, amount of catalyst loading, aeration rate, and the initial concentration of RR4 dyes were found to influence the pseudo-first order rate constant of the photocatalytic activities of RR4. The presence of aeration as oxygen source promoted the photocatalytic removal. The optimum catalyst loading was determined at $1.500 \pm 0.005 \text{ mg cm}^{-2}$ and the photocatalytic degradation of RR4 was highest at acidic condition. The increase of the initial concentration of the RR4 dyes decreased the degradation rate. The role of adsorption and the chemical structure of the organic pollutants affected the photocatalytic degradation rate. The degradation rate for RR4 and phenol were much

slower using immobilized system. However for the degradation of MB, immobilized system was found to be much faster than the suspended system. The immobilized P-25/ENR/PVC/5h catalyst plate can be reused for many repeated cycle of applications. The mineralization of organic pollutants was also evaluated by measuring COD, the changes of pH of the solution, and the evolution of nitrate, sulphate and chloride anions of the pollutants. It was observed that the decolorization process of the RR4 and MB dyes were always faster than their mineralization process, however the decomposition of phenol was almost identical with their mineralization process.

CHAPTER 1

INTRODUCTION

1.1 An Overview

Approximately 2 over 3 parts of our Earth's surface is covered by water. Although, the water is apparently abundant, we have only less than 1 % of the world's fresh water accessible for direct human and all other living creatures' use [1]. The remaining of Earth's water comes from the salty oceans water and the rest is frozen in the form of polar ice sheets or glaciers. Fortunately, Malaysia receives abundant rainfall annually. However, because of our life revolves around water, a sufficient clean water is essential for our healthy living as well as the health of the environment. Besides that, in the coming years, the consumption of clean water is expected to increase due to the global expansion of industrial activity as well as population growth.

Even though the accessibility of clean water has emerged as one of the most serious problem in twenty-first centuries, we as humans still disregard it by polluting our rivers, lakes and oceans. Currently, most of these sources are contaminated, more or less, with a great variety of organic and sometimes inorganic pollutants that can be dangerous to public health. In order to resist water pollution, we must understand the problems and become part of the solution. Water pollution occurs when any pollutants are discharged directly or indirectly into water bodies without specialized treatment to remove harmful components. Thus, water pollution can be described as any chemical, physical, or biological change in water quality that makes it unusable or causes harm to ecosystems [2]. According to statistics compiled by the

Department of Environment (DOE) in 2006, about 47.79 % of water pollution point sources in Malaysia come mainly from sewage treatment plants, followed by manufacturing industries (45.07 %), animal farms (4.58 %) and agro-based industries (2.55 %) [3]. This reveals that the increasingly sophisticated lifestyles, rapid industrialization, and intensive farming pollute our water bodies.

Usually, the pollutant effects are greater near to their source, but pollutants may have effects far from their sources too because wastewater will migrate. In addition, the decomposition of harmful organic content in wastewater will produce many unknown intermediates which are more toxic than the original compound. Hence, the hazardous wastewater released to the streams is dangerous because it can kill life that inhabits water-based ecosystems [4]. This in turn can harm the birds and other animals that eat this contaminated food supply. Therefore in general, water pollution can disrupt the natural food chain. Furthermore, water pollution gives detrimental effects on humans such as hepatitis, diarrhoea, skin lesions, and cancer by eating seafood that has been poisoned [5].

Therefore, it is a major challenge for us to find viable solutions to the growing shortage of clean water. We cannot prevent the pollution or achieve zero-wastewater, because pollutants will be continuously produced since there is no process that is 100 % efficient. One way to reduce the water contamination is by minimizing the amount of pollutants produced at the source. However, the most effective way to remove contamination from polluted water is by wastewater treatment.

1.2 Organic Pollutants in Wastewater

The usage of organic chemicals for industrial, agricultural, and domestic applications has been widespread and gives a lot of benefits to the users. Unfortunately, many chemicals will contaminate our water bodies either as a consequence of discharges of wastewater or run-off from urban and agricultural areas. Basically, the chemical composition in the wastewater strongly depends on its origin. Besides that, the chemicals that have found their way into the water cycle are known and suspected to be carcinogenic and dangerous to public health. Usually, waste materials like toxic metals, oil, grease, dyes, pesticides, herbicides, surfactant, and even radioactive materials are discharged into the water bodies and considered as relatively common pollutants from farms, households, and industries. However, there are mainly two types of wastewaters that are of heightened concerns over public health which are those that contain coloured and phenolic compounds.

1.2.1 Coloured wastewater

Dyes are the molecules that produce colour and absorb intensely in the part of the electromagnetic spectrum [6]. Over 100,000 different dyes have been applied in pulp and paper, food, cosmetic, colour photography, pharmaceutical, and textile wet processing industries [7-10]. The majority of dyes used are synthetic dyes which usually are derived from two sources namely coal tar and petroleum-based intermediates. Synthetic dyes also have become common water pollutants and are usually found in trace quantities in industrial wastewater owing to their good stability in water [11]. Wastewaters originated from dye production and their applications are usually the first contaminant to be identified because they are highly visible and

present a very serious environmental problem even in very small amount because of its impact on the aesthetic nature of the environment.

Nowadays, reactive synthetic dyes are predominantly used among all dyes for dyeing cotton, wool and other cellulose fibers [9]. Almost 70 % of the reactive synthetic dyes are mainly azo type and the rest are anthraquinonic and phtalocyanine types [10]. Reactive azo dyes are extensively used because their reactive groups allow the covalent bond to be formed with cellulosic and protein fibers [9]. The utilization of azo dyes poses a major carcinogenic potential due to the possibility of forming certain aromatic amines (notably benzidine) in their breakdown in the environment [12].

Azo dyes can be classified as acid dyes (anionic) or basic dyes (cationic). Acid dyes are characterized by having sulfonic acid group attached to the aromatic ring of the dye molecule and give them negative charges [13]. These acid dyes are commonly used in wool and nylon dyeing industries because the amino group in these fibers become protonated and have a positive charge in acidic condition, thus attracting the negatively charged dye anions [14]. In contrast, basic dyes usually have amino group that are positively charged. The negatively charged fibers such as polyester and acrylic will be attracted to the positively charged cationic dyes [14].

Approximately 15 % of the total world production of dyes have been lost during manufacturing and processing operations and then released to the environment through industrial effluents [11]. Strict restriction is imposed on the organic compositions of industrial effluents due to the carcinogenic and mutagenic

properties of some types of dyes. Thus, it is essential to eliminate the hazardous compound in dyes from effluents before they can be discharged into the environment. However, the process of their decolorization is deemed difficult due to the complex structural varieties of the dyes and their synthetic origins.

1.2.1.1 Reactive Red 4, RR4

Reactive red 4 (RR4) or also known as Cibacron brilliant red 3B-A is classified as an anionic monoazo dye since this dye possesses only one nitrogen to nitrogen double bonds (-N=N-) that are usually attached to two radicals of aromatic groups (benzene or naphthalene rings) as shown in Figure 1.1. The colour of RR4 dyes is determined by the azo bonds and their associated chromophores (sulfonate group) and auxochromes (hydroxyl group). This triazine-containing group azo dye is known to be resistance towards light due to the presence of the s-triazine and is commonly used for dyeing cellulose, nylon, silk, and wool. It is hydrophilic in nature, and is widely used in food, drugs, cosmetics and inks [15].

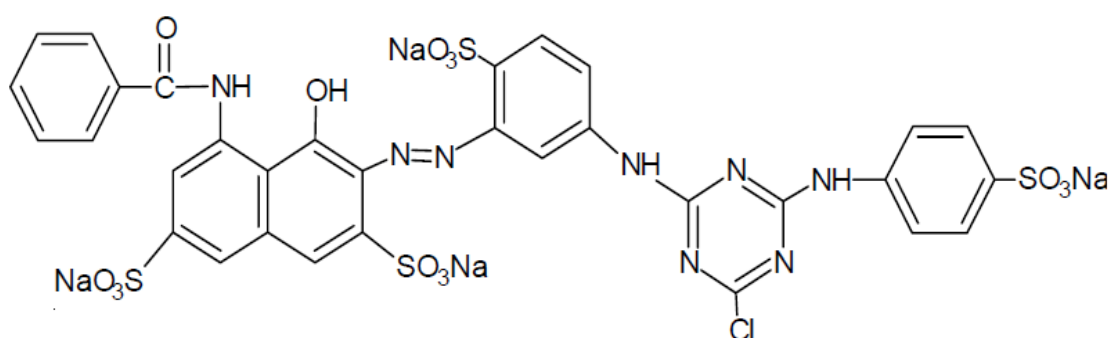


Figure 1.1: Molecular structure of RR4 dye

The RR4 dye has a strong absorption in the visible light at λ_{max} 517 nm. Due to their toxicity and slow degradation, these dyes are classified as environmentally

hazardous materials. This dye has been chosen as the first model pollutant because it is one of the major pollutants found in wastewater released by textile and leather industry. Apart from that, the photophysical aspects of this dye can be easily studied by spectrophotometry in the visible spectral range. Furthermore, it will be interesting to look into the photocatalytic induced chemical processes that occur upon a large molecule dye with huge chemical structure such as RR4.

1.2.1.2 Methylene Blue, MB

In an attempt to evaluate the versatility of the prepared immobilized photocatalyst, methylene blue (MB) was employed as the cationic dye model pollutant. MB is a cationic thiazine dye and is also known as a C. I. Basic Blue 9 with a molecular formula of $C_{16}H_{18}N_3SCl$. MB is one of the popular choice of dye for assessing photocatalytic activity because it is highly coloured, inexpensive and has a strong adsorption in the visible region ($\lambda_{max} = 661 \text{ nm}$) which is easier to detect for decolorization test. Besides that, MB also does not absorb strongly in the UVA region and so it is reasonably stable photochemically under UVA irradiation [16]. At room temperature, it appears as a solid, odourless, dark green powder, which yields a blue solution when dissolved in water. This dye is commonly applied for dyeing cotton, wool, silk, and leather [17]. Besides that, it is also used for acrylic fibers, paper, cosmetics, and in ink printing [15]. For medical application, MB is a basic dye commonly used in histologic, microbiologic and tissue staining [17]. Its release into the ecosystem causes water bodies to become coloured, absorbing and reflecting sunlight, which in turn interferes with the aquatic ecosystem and may cause chronic and acute toxicity.

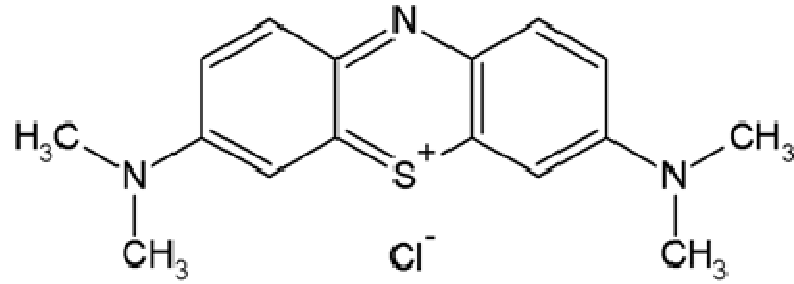


Figure 1.2: Molecular structure of MB

1.2.2 Phenol compounds

Other most common organic water pollutants are phenolic compounds which are toxic even at low concentration. Phenol with the chemical formula C₆H₅OH exists naturally and is manufactured in large quantities. It is found naturally in some foods, in human and animal wastes. Besides that, phenolic compounds could also be produced from decomposition of organic matter in aquatic environment, such as algal secretion, lignin transformation, hydrolysable tannins and flavanoids, and human humidification processes at low concentration [11,18]. Moreover, these compounds are also released into the environment from effluents discharged by a variety of industries, such as petroleum refining, coal tar, chemical synthesis, synthetic resins, dyestuff, coke plants, paper and pulp mills and pharmaceuticals as well as pesticides and herbicides manufacturers [11,19,20]. Furthermore, the presence of phenol and their derivatives in wastewater can lead further to the formation of substituted compounds during disinfection and oxidation processes. They also induce genotoxic, carcinogenic, immunotoxic, haematological and physiological effects. In addition, high bioaccumulation rate occurred along the food chain due to its lipophilicity [21].

Due to their solubility in water, phenol becomes one of the most common organic water pollutants because it can migrate swiftly through aquifers and cause widespread contamination in both surface and groundwater. Phenol is toxic even at low concentrations and also the presence of phenol in natural water can lead further to the formation of substituted compounds during disinfection and oxidation [22].

Further, this compound has toxicity and carcinogenic characters and quite stable and stays in the environment for longer period of time, thus they can directly impact the health of ecosystems and present a threat to humans through the contamination of surface or ground water. Therefore, there is a need for an effective and economic wastewater treatment of industrial effluents containing phenolic compound before it gets discharged into the water bodies.

Besides that, phenols are well known for their bio-recalcitrant and being introduced continuously into the aquatic environment through various anthropogenic inputs [23]. Therefore, their toxicity and persistence can directly impact the health of ecosystem and present a threat to humans through contamination of drinking water supplies. Repeated exposure to low levels of phenol in drinking water has been dissociated with diarrhea and mouth sores in humans [22]. Ingestion of very high concentration of phenol also has resulted in death [22].

Adsorption process over activated carbon is the most popular method and widely used to remove phenol from water bodies [24]. However, by heterogeneous photocatalysis approach, it is expected to be more environmental friendly, as they

can lead to complete mineralization or formation of non-toxic residues of noxious organic waste at low cost.

1.3 Decomposition of Organic Pollutants in Wastewater

Due to the complexity and the variety of organic pollutants contaminating the water ways, manufacturers and users of chemical substances have faced increasingly stringent legal regulations in order to protect human health and the environment. However, to treat a large volume of effluent is a very costly process and investment in effluent treatment is often considered as a waste of money as it makes no contribution to their profit. To fulfil those requirements, new technologies need to be designed, specifically, to analyze and remove the hazardous pollutants from wastewater effluents. In addition, on-site wastewater treatment is needed to prevent the formation of more hazardous compounds when all of the various sources of organic contaminants mix together in water bodies.

1.3.1 Wastewater treatment methods

A variety of physical, chemical and biological methods are available for wastewater treatments. However, in the beginning of the 1970's, only physical treatment methods were applied to maintain the pH, total dissolved solid, and total suspended solid of the discharged water [9]. At this time, no obligatory discharge limits for the colour effluents was implemented. Physical methods of wastewater treatment include different precipitation methods (coagulation, flocculation, and sedimentation), adsorption (on activated carbon, biological sludge, and silica gel), filtration, and reverse osmosis.

The applications of activated carbon to phenolic adsorption have been reviewed recently [24]. However, the adsorption capacity of activated carbon for aromatic compounds depends on a number of factors such as the physical nature of the adsorbent, the nature of the adsorbate, and the solution conditions. The shortcoming in this process is that there is no chemical transformations occurred. Therefore, they are generally involved in transfer of waste components from the liquids phase to a sludge phase [20]. That makes them insufficiently effective and moreover very expensive due to the required further treatment of the generated secondary waste and also due to the regeneration of inactive adsorbents after used.

Tanaka et al. [25] reported that the adsorption capacity for some of the reactive dyes on activated carbon is relatively low. Besides that, various natural organic materials were used to remove reactive dyes by adsorption process such as plant residues, known as biomasses, which include cellulose, sugarcane bagasse, rice husk, and coconut husk, which are alternatively cheaper adsorbents [9,10]. Furthermore, coagulation and flocculation processes using Fe(III) and Al(III) salts showed high efficiency for decolourization of coloured wastewater [26]. Nevertheless, the main problems of this relatively cheap and easily maintained treatment process are correlated with the generation of large amount of sludge as a secondary waste which requires further treatment [27].

Biological treatment methods are also widely applied for the municipal and industrial wastewater treatments. This treatment can be conducted in the presence or absence of oxygen. Even though the presence or absence of oxygen, have proven to be adequate, but certain dyes can inhibit bacterial development thus reducing their

efficiency [28]. Therefore they cannot be successfully applied for the treatment of coloured wastewater containing reactive dyes due to their poor biodegradability caused by their recalcitrant nature [9]. In addition, approximately 53 % of the dyes used are resistant to microbial attack [12, 14].

Recently, several azo-reducing bacteria, including *Rhizobium radiobacter* [13], *Pseudomonas* [29], *Candida rugopelliculosa* [30] and *Bacillus lentus* [31] are found to decolorize and mineralize some of the reactive azo dyes. However, biological process by itself is often inappropriate due to the low rates of biological degradation. In addition, the application of this method in wastewater treatment containing phenolic compound is not convenient due to its toxicity that may cause the phytotoxic effect on the active microorganisms which makes the degradation rate to become slower [18].

In chemical treatment, the most widespread application for wastewater treatment is by using chlorine and ozone. In chlorination process, sodium hypochloride, NaOCl is used for decolourizing wastewater. However, the main disadvantage in this process is the concern about the production of chlorinated organic compounds that are in most cases even more toxic and carcinogenic than the parents' contaminants [9, 32]. Moreover, the application of chlorine in wastewater treatment is characterized as a low selectivity and high consumption method. Ozone process is much more effective as a disinfectant than chlorine, but their problem include its instability and its hazardous nature due to the strong and non-selective oxidizing power [33]. Therefore, a post treatment destruction unit must be used to prevent unreacted ozone from escaping into the atmosphere. As reported by O.

Gimeno et al., [34], the destruction of chromophoric structure of the dyes by the ozonation process is effective but often a complete mineralization is not achieved.

From the previous discussion, all of these processes have some advantages and disadvantages over each other. However, it is apparent that the elimination of the contaminants using a single treatment method cannot be achieved. Furthermore the combination of two or more wastewater treatment methods is quite a challenge. It is therefore essential to investigate alternative efficient methods to remove highly toxic compounds from potential sources of clean water. Recently, the emergence of advanced oxidation processes (AOPs) has been a considerable interest to scientists as attractive alternative technologies for destroying toxic organic contaminants.

1.3.2 AOP methods

AOPs methods are based on the generation of very reactive and oxidizing free radicals that have been used with an increasing interest due to their high oxidant power. This process involves the production of reactive hydroxyl radical (OH^\bullet) that are ultimately capable in destroying organic chemicals that result with the mineralization of organic pollutants into CO_2 , H_2O and simple mineral acids [8, 11, 18, 27, 34]. Besides that, OH^\bullet radical is a non selective chemical oxidant due to its higher oxidation potential (E°) of 2.80 V, compared with 2.07 V for ozone, 1.50 V for chlorine dioxide, and 1.36 V for chlorine, and reacts very rapidly with most substances because of its unpaired electron [35]. AOPs show high flexibility in their practical applications because they can be used either separately or in combination with two or more AOPs methods. Several methods are available in AOP that can be

classified as a non-photochemical and photochemical process and are summarized in Table 1.1.

Table 1.1: An established and emerging AOP methods [36]

Process	AOP systems
Non-photochemical	O ₃ /H ₂ O ₂
	Ozonation catalysis, O ₃ /Cat
	Fenton, H ₂ O ₂ /Fe ²⁺
	Fenton-like, H ₂ O ₂ /Fe ²⁺ -solid
Photochemical	O ₃ /UV
	H ₂ O ₂ /UV
	O ₃ /H ₂ O ₂ /UV
	Photo Fenton, H ₂ O ₂ /Fe ²⁺ /UV
	Heterogeneous catalysis/UV

1.3.2.1 Non-photochemical processes

In O₃/H₂O₂ system, the addition of hydrogen peroxide, H₂O₂ and ozone, O₃ into a wastewater sample can accelerates the decomposition of O₃, thus resulting in the formation of OH[•]. However, the performance of this process depends on the O₃ dose, contact time, and the alkalinity of water [36]. Another approach in order to accelerate ozonation reactions is by using heterogeneous or homogeneous catalysts. Several metal oxides or metal ions that are usually used as a catalyst in this process are Fe₂O₃, Al₂O₃-Me, MnO₂, Fe²⁺, Mn²⁺, and so on [36]. However, the usage of O₃ typically requires an air permit for O₃ emissions in addition to an off-gas treatment system for O₃ destruction. Besides that, the treatment for excess H₂O₂ may be

required because it can serve as an oxygen source for microorganisms and can promote biological re-growth in the distribution system.

In Fenton and Fenton-like system, radicals including OH^\bullet are produced when Fe(II) ion or heterogeneous metal supported system (use in Fenton-like system) reacts with H_2O_2 . Thus, destruction of organic matter occurs by reaction with these radicals. The reactivity of this system was first observed by Fenton in 1879 [35, 36]. This process is quite attractive because it can degrade many types of organic pollutants such as phenols, formaldehyde, pesticides, wood preservatives, and plastics additives [5,30,37]. Besides that, non-toxic iron is highly abundant and H_2O_2 is easy to handle and environmentally benign. However, the regeneration of catalyst is very slow, therefore continuous addition of Fe(II) ions is needed in order to sustain the reaction. In addition, this reaction is only effective at low pH range in order to keep the iron in solution [35], thus pH adjustment procedure will increase the cost of operation and maintenance.

1.3.2.2 Photochemical process

In O_3/UV system, the photolytic ozonation process is more effective for the destruction of some organic compounds compared with UV-photolysis or ozonation alone. In this process, OH^\bullet are generated when low pressure UV light is applied to the ozonated water. Destruction of organic compounds occurs by OH^\bullet reactions, coupled with direct photolysis and oxidation by molecular O_3 . However, the turbidity and colour of the wastewater can obstruct the penetration of UV light, thus lowering their efficiency. Besides that, the application of O_3 in wastewater treatment is limited due to its high energy demand [38].

In $\text{H}_2\text{O}_2/\text{UV}$ system, under UV irradiation, H_2O_2 molecules are photolyzed to form two OH^\bullet radicals that will react with organic substances. A disadvantage of this process is the utilization of solar light as the source of UV light which is limited due to the fact that the required UV energy for photolysis of the oxidizer is not available in the solar spectrum [39]. Moreover, the application of H_2O_2 in this system for the treatment of drinking water was unlikely to be practical because the accumulation of H_2O_2 would occur within the treated water.

The application of $\text{O}_3/\text{H}_2\text{O}_2/\text{UV}$ process is not so widely investigated especially for the treatment of wastewater containing reactive dyes. This method is a combination of $\text{H}_2\text{O}_2/\text{UV}$ and O_3/UV system. There are several ways to generate OH^\bullet which include photolysis of formed H_2O_2 or by reaction between formed H_2O_2 and O_3 . The addition of H_2O_2 to the O_3/UV process accelerates the decomposition of O_3 , which results in an increased rate of OH^\bullet generation. However, the capital and operating costs for the UV/O_3 and/or H_2O_2 systems vary widely depending on the wastewater flow rates, types and concentration of pollutants present, and the degree of removal required [36].

The addition of UV into the Fenton process can improve the oxidation efficiency by enhancing both catalyst regeneration and hydroxyl radical formation. The presence of UV can generate additional OH^\bullet radicals from the photolysis of H_2O_2 besides the primary source throughout the reduction of $\text{Fe}(\text{II})$ ions in the mechanism of the Fenton process. Heterogeneous catalysis/UV system or also known as a heterogeneous photocatalysis is a part of the AOP system which is proven to be a promising technology for the degradation of organic compounds. This technique is

more effective in comparison with other AOPs because of the utilization of inexpensive semiconductor and capable to mineralizing various organic and inorganic compounds [9, 27]. The basis of photocatalysis is the photo-excitation of a solid semiconductor as a result of the absorption of UV irradiation that produces conduction bands electron and valence band holes. These charge carries are able to induce reduction and oxidation processes thus degrading organic molecules. A detail discussion about this technique is provided in the Section 1.4.

1.4 Fundamentals of Heterogeneous Photocatalysis

Research on the heterogeneous photocatalysis started growing rapidly since 1972, after Fujishima and Honda discovered the photocatalytic splitting of water using TiO_2 electrodes, [40, 41]. Many applications of this technique have been implemented in many fields such as industrial, environmental cleanup, and health applications. In the United State, TiO_2 -coated glass microbubbles have been developed for the specific application of cleanup of oils films on water [41].

Besides that, another applications blessed with the heterogeneous photocatalysis is self cleaning function [42]. Thereby, a combination of the effects of photocatalysis and superhydrophilicity is used and markedly widened the application range of heterogeneous photocatalysis. Afterwards, the dirt can be easily removed by the complete wettability of the surface with water [41, 42]. In anti-fogging function, the application of TiO_2 in heterogeneous photocatalysis can be applied for surfaces like mirrors, glasses, or showcases. In this process, the formation of water droplets is suppressed by superhydrophilicity of TiO_2 .

Later, synthesis, processing, and characterization of new semiconductor materials become the main interests, connected to industrial processes. Nowadays, the main goal of research and development in the area is the use of the technique for air purification and wastewater treatment. In this way, organic and inorganic compounds and even microorganisms and trace metals are degraded or transformed into less harmful substances. The removal of trace metal such as mercury (Hg), chromium (Cr), lead (Pb), arsenic (As) and other toxic metals are essentially important for human health and water quality. Thus, as reported by Herrmann et al.[44], the removal of toxic metals can be achieved by semiconductor photocatalytic process. Besides that, the photoreducing ability of photocatalysis has been used to recover expensive metals from industrial effluent, such as gold, platinum, and silver.

In addition, photocatalysis has been used for the destruction of organic compounds such as alcohols, carboxylic acids, phenolic derivatives, or chlorinated aromatics [11]. Herbicides and pesticides that may contaminate water also can be mineralized through heterogeneous photocatalysis [43, 45]. Therefore, heterogeneous photocatalysis is more interesting than conventional methods because the former gradually breaks down the contaminant molecules with no residues of the original material remain, and consequently no sludge produced.

Photocatalytic reactions are usually initiated through electronic excitation of a semiconductor caused by light absorption that drastically alters its ability to lose or gain electrons, which subsequently led the pollutants to be degraded into harmless by-products [9, 27, 33]. Moreover, this destructive process does not involve mass transfer, can be carried out under ambient conditions, and may lead to complete

mineralization of organic carbon into CO₂, H₂O and mineral acids [33, 45]. The catalyst itself is unchanged during the process and no consumable chemicals are required. Taken together, these advantages of heterogeneous photocatalysis resulted in considerable savings in the wastewater treatment costs while keeping the environment clean.

1.4.1 Photocatalysts

Photocatalytic degradation involves the use of certain semiconductors as catalysts for the production of the OH[•] radicals and has proven to be an effective method for wastewater treatment without having any of the certain drawbacks as mentioned before. A good photocatalyst should possess some essential characteristic: (i) photoactive, (ii) light absorption should occur in the near UV and possibly in the visible wavelength ranges, (iii) biologically and chemically inert, (iv) the stability should be such that its re-utilization is possible (not prone to photo-corrosion), (v) inexpensive, and (vi) non-toxic [46]. Besides that, the energy associated with the valence band, E_v must allow the formation of species that are able to oxidize most organic molecules. In addition, the recombination rate of electrons and holes should be relatively low so that the photogenerated charges can migrate to its surface and give rise to redox processes with appreciable rates [47].

Si, TiO₂, ZnO, WO₃, CdS, ZnS, SnO₂, and Fe₂O₃ are among the preferred semiconductors which can be used as photocatalysts. The ability of a semiconductor to undergo photo induced electron transfer from the valence band to the conduction band after being illuminated with light is governed by the band energy positions of the semiconductor and the redox potential of the organic molecules. The band gap

energy, E_{bg} is referred to the distance between the occupied valence band and the unoccupied conduction band in the band structure of the semiconductor. Figure 1.3 reports the bands gaps positions of the valence band and the conduction band edges for various semiconductors together with some selected redox potentials.

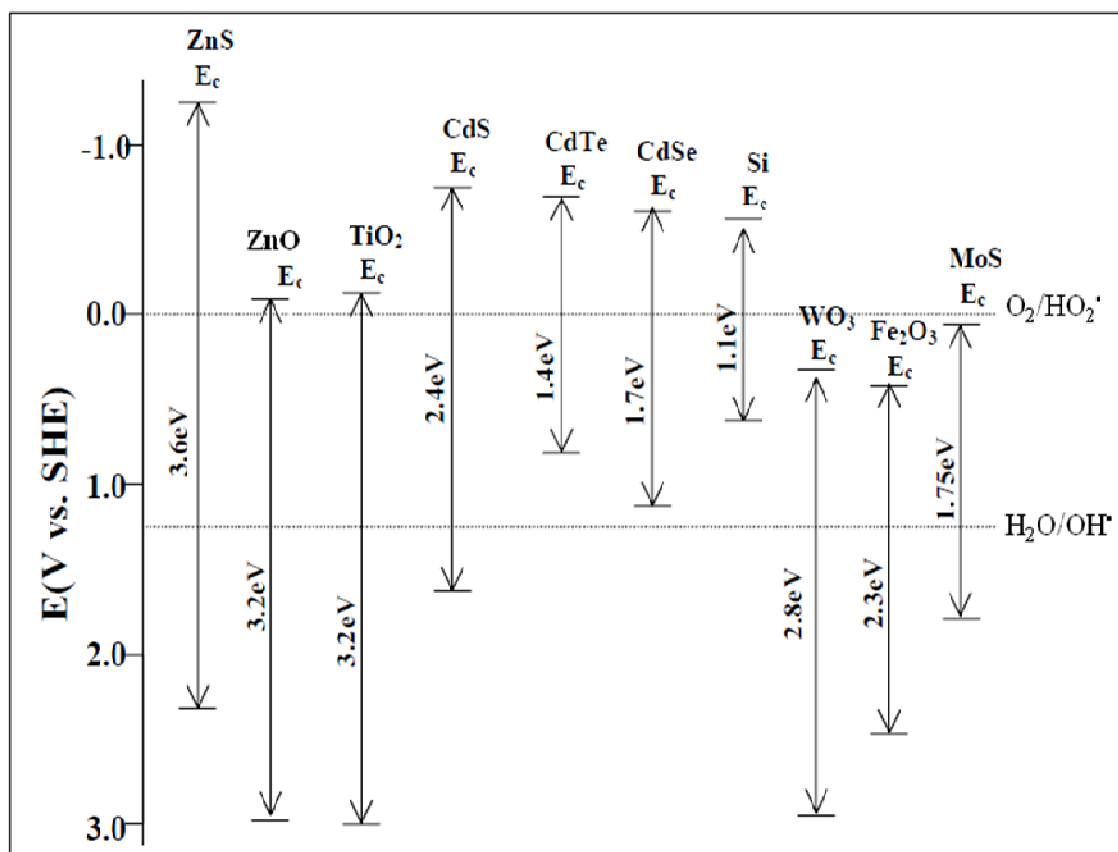


Figure 1.3: The conduction and valence band positions of the selected semiconductors at pH 0. [Picture adapted from 47, 48]

The energy level of the conduction band edge, E_c corresponds to the reduction potential of photoelectrons. Likewise, the energy level of the valence band edge, E_v corresponds to the oxidizing ability of photoholes [47]. Therefore, each value is represents the ability of the system to promote reduction and oxidation processes. Figure 1.3 shows the redox potential of the H_2O/OH^* and O_2/HO_2^* couples. If the E_v

of the semiconductor is more positive than the potential of the species present in the solution, the photogenerated holes will have sufficient energy to oxidize the organic substances via the generation of OH^\bullet [46, 47].

Thus the redox potential of the organic species must lie within the band gap position of the photocatalyst as exemplified by ZnS, ZnO, TiO_2 , and CdS as shown in Figure 1.3. However, due to the photo instability of ZnO with respect to its inappropriate dissolution to yield $\text{Zn}(\text{OH})_2$ on the ZnO particle surfaces, lead to the catalyst inactivation that hindered the utilization of ZnO as photocatalyst [46, 49]. Besides that, the usage of ZnO and CdS will suffer from the photocorrosion induced by the self-oxidation. Furthermore, the competing reactions between ZnO and CdS with generating holes lead to the decrease in the production of OH^\bullet radicals, thus lowering the photodegradation rate [49, 50].

Nepollian et al. [49] reported that the CdS are less active in comparison to TiO_2 for degradation of dyes. Hence, CdS cannot be applied in real wastewater because the occasional release of metal ion (Cd^{2+}) into the aqueous medium may cause heavy metal pollution. Moreover, the application of metal sulphide semiconductors is unstable since they undergo photoanodic corrosion, while Fe_2O_3 will undergo photocatodic corrosion. Generally, the application of TiO_2 in a photocatalytic process proceeds without having any shortcomings and can mineralize a wide range of organic pollutants that includes aliphatic, aromatics, detergents, dyes, pesticides, and so on [9, 14, 25, 45]. Moreover, nanostructures of TiO_2 photocatalysts is currently receive great attention because it is largely available,

inexpensive, non-toxic, and shows relatively high chemical stability in comparison to other semiconductors [41, 42, 46, 47].

1.4.2 Titanium dioxide (TiO₂) as a semiconductor

1.4.2.1 Historical background

Titanium dioxide also known as titanium (IV) oxide with the molecular weight of 79.87 g mol⁻¹ is the naturally occurring oxide of titanium. Titanium is the world's fourth most abundant metal (exceeded only by aluminium, iron, and magnesium) and the ninth most abundant element. It was discovered in 1791 in England by Reverend William Gregor, who recognized the presence of a new element in ilmenite [40]. In the beginning of the 20th century, industrial production started with TiO₂ production replacing toxic lead oxides as a pigment for white paint. Significantly, TiO₂ has been used as white pigment from ancient times and thus, its safety to humans and the environment is guaranteed by history [41].

Fujishima and Honda were the first to discover the ability of TiO₂ in splitting water under UV light in the early 1970s [51]. They revealed the possibility of water splitting by photo electrochemical cell using a rutile TiO₂ photoanode and platinum (Pt) as a counter electrode [40, 47]. Since then, TiO₂ has drawn great attention to researchers in the field of photovoltaic and photocatalysis. With time, the research shifted to the utilization of TiO₂ for the destruction of organic and inorganic pollutants. Carp et al. [40] reported that, in 1977, Frank and Brad were the earliest to report about the application of TiO₂ in environmental purification by examining the photolytic decomposition of cyanide in water. Furthermore, Hashimoto et al. [41] state that, in the 1980s, the detoxification of various harmful compounds into CO₂ was

demonstrated by T. Inoue using TiO_2 powder. These accomplishments subsequently attracted more interests in the application of TiO_2 as a photocatalyst.

TiO_2 is industrially produced by two basic processes. Both of these processes use mineral ilmenite (FeTiO_3) as the raw material. The first is a sulphate technology, where ilmenite is leached by sulphuric acid and engendering TiOSO_4 is decomposed by steam to TiO_2 [40, 48]. The second process is chloride technology (used in Degussa for production of P-25) which is based on chlorination of ilmenite to produce TiCl_4 . After purification, TiCl_4 was oxidised by oxygen to produced TiO_2 [40, 48].

1.4.2.2 Structural and photocatalytic properties of TiO_2

Currently, TiO_2 production exceeds 4 million tons annually [40]. Most of the TiO_2 pigments in industries are produced from the titanium material either by sulphate or chlorine process. TiO_2 has a wide range of applications. The major utilization of TiO_2 as a white pigment is in paints, plastic, and paper production sectors. However, the consumption of TiO_2 increased due to the development in minor end-use sectors such as textiles, food, leather, and pharmaceuticals (tablet coatings, toothpaste, and as a UV absorber in sunscreen cream with high sun protection factors and other cosmetic products) [40, 48]. In addition, due to the high refractive index, it is used as anti-reflection coating in silicon solar cells and in many thin-film optical devices [45]. TiO_2 is also successfully used as a biomaterial due to its hemo-compatibility with human body as bone substituent and reinforcing mechanical supports.

In nature, TiO_2 occurs in three different forms namely as rutile, anatase and brookite minerals [52]. The structures of rutile, anatase and brookite can be described in terms of octahedral (TiO_2^{6-}) unit. In these structures, the basic building blocks consist of a titanium atom which is surrounded by six oxygen atoms. These three crystal structures also differ by the distortion of each octahedral and by the assembly patterns of the octahedral chains [40, 48]. In rutile form, the octahedra are linked by sharing an edge along the c-axis to form chains. Conversely in anatase, it was built up from octahedra that are connected by their vertices [40]. In brookite, the octahedra share both edges and corners, forming an orthorhombic structure.

However, the photocatalytic activity of these three structures depends on the crystalline structure, the surface area, and the particles distribution. The high band gap energy for anatase ($E_g = 3.2 \text{ eV}$) and rutile ($E_g = 3.0 \text{ eV}$) phases allows us to utilize only radiations with a wavelength lower than 390 nm [5, 40]. Although the position of valence and conduction bands of both anatase and rutile are positive enough to allow the oxidation of many organic molecules, it has been pointed out that the photodegradation rate is much more rapid over anatase than rutile TiO_2 . The poor efficiency of rutile is mainly due to the high recombination rate of electron-hole pairs created when TiO_2 is illuminated with light [46]. Moreover, rutile TiO_2 has low ability to photo-adsorb oxygen [5]. TiO_2 brookite phase has been used less frequently in photocatalysis system because it only can be obtained as a mixture with one or both of the other phases and its separation implies an additional peptization process [48]. Besides that, brookite is only stable at very low temperature and thus it is not suitable in photocatalytic applications.

1.4.2.3 Titanium Dioxide Degussa P-25

A number of commercially available TiO₂ catalysts have been investigated for the photocatalytic degradation of various types of pollutants in aqueous environment. The photocatalyst titanium dioxide Degussa P-25 (known as P-25) has been widely used in most of the experimental conditions than other commercial catalyst powder, such as Hombikat UV-100 (Sachtleben Chemic Gmbh), TiO₂ – PC 500 (Mellenium Inorganic Chemicals), TiO₂ – Tytanpol A11 (Police Company, Poland) for the photocatalytic degradation of toxic compounds. P-25 contains 70 – 80 % of anatase and 30 – 20 % of rutile phase with a specific Brunauer Emmett – Teller (BET) surface area of 55 m²g⁻¹ [53]. The photocatalyst PC 500 has a BET surface area of > 250 m²g⁻¹ with 100 % anatase [53].

It has been demonstrated that the degradation rate of organic compounds occurs much more rapidly in the presence of P-25 in comparison with PC 500 catalyst [53-55]. However, Bizani et al. [33] reported that Hombikat UV-100 appeared to be more effective on dye oxidation than P-25. Hombikat UV-100 was more efficient due to its large BET surface area which is 250 m²g⁻¹. Zielinska et al. [56] made a comparison between the photocatalytic degradation of various organic dyes using Tytanpol A11 (100 % anatase) and P-25 under UV-Vis illumination. The degree of decomposition of organic dyes was lower for Tytanpol A11 than P-25 catalyst in all cases. This was due to the surface area of P-25 which was almost 5 times higher than Tytanpol A11 catalyst. Besides that, the band gap energy of P-25 was 0.17 eV lower than for Tytanpol A11.

It is widely accepted that the TiO₂ anatase is more effective in photocatalytic degradation than the rutile TiO₂ because the former has higher adsorptive affinity for organics and have superior hole-trapping ability. However, it has been shown that a commercialized mixture of two phases (Degussa P-25) exhibit much more superior photocatalytic degradation than pure anatase TiO₂. Ohno et al., [57], found that the presence of both anatase and rutile phases was important in photocatalytic reactions where oxygen was used as an electron acceptor.

In fact, the enhanced activity in mixed-phase catalysts results from prolonged separation of photogenerated electrons and holes through interfacial electron transfer from the conduction band of rutile phases to the trapping states of anatase phase thus giving its synergistic effect [23, 58]. In this mixed-phase material, pure rutile which is relatively inactive due to the high rates of recombination of electron and holes will shift the photo response of anatase phase into the visible light region and increasing the photocatalytic activity by hindering charge recombination [59]. This phenomenon was proven by Wahi et al., [58] and Li et al., [59], whom systematically prepared the mixed-phase photocatalyst in order to explain the superior photocatalytic activity of Degussa P-25. However, Bhatkhande et al [46] suggested that the electron at the conduction band of the anatase part jumps to the conduction band of rutile part which is less positive. This allows the hole to move to the surface of the particle and the recombination of electrons and holes is thus prohibited.

1.5 Mechanism of Photocatalytic Oxidation Process

Usually it is assumed that oxidative and reductive photocatalytic reactions take place simultaneously on TiO₂ particles. The adsorption of radiation at suitable